

# Two-Particle Microrheology of quasi-2D Viscous Systems

V. Prasad, S. A. Koehler, and Eric R. Weeks

*Department of Physics, Emory University, Atlanta, GA 30322*

(Dated: February 6, 2008)

We study the spatially correlated motions of colloidal particles in a quasi-2D system (Human Serum Albumin (HSA) protein molecules at an air-water interface) for different surface viscosities  $\eta_s$ . We observe a transition in the behavior of the correlated motion, from 2-D interface dominated at high  $\eta_s$  to bulk fluid-dependent at low  $\eta_s$ . The correlated motions can be scaled onto a master curve which captures the features of this transition. This master curve also characterizes the spatial dependence of the flow field of a viscous interface in response to a force. The scale factors used for the master curve allow for the calculation of the surface viscosity  $\eta_s$  that can be compared to one-particle measurements.

PACS numbers: 83.10.Mj, 87.68.+z, 87.16.Dg

Diffusion in three dimensions has been well understood since 1905, when two authors showed that the motion of particles suspended in a fluid is related to the fluid's viscosity [1, 2]. This observation has been generalized in a technique called microrheology, which measures the thermal motion of tracer particles introduced in a viscoelastic material. From the motions of the particles, the material dependent properties can be determined, such as the elastic modulus,  $G'(\omega)$ , and the viscous modulus,  $G''(\omega)$  [3]. This has been applied to measure the viscoelasticity of bulk materials such as polymer solutions [4], biomaterials [5] and hydrogels [6]. A closely related question is the motion of tracer particles in a two-dimensional system such as lipid molecules at an air-water interface [7] or lipid rafts in cell membranes [8]. For example, in a purely viscous 2-D system, one might imagine that the diffusive properties are related to the two-dimensional viscosity, and that by following the motion of tracer particles one could determine this viscosity. However, in most cases of practical interest, a strictly two-dimensional surface is an idealization and in reality the surface is adjacent to three-dimensional fluid reservoirs. For example, recent experiments study diffusion in biological systems such as cell membranes [8, 9] which are surrounding a 3-D cell and immersed in a 3-D fluid. This coupling modifies the behavior of tracer particles and makes interpretation of the results trickier [10, 11, 12].

Furthermore, in many cases in 3D, tracers are known to modify the structure of the medium in their vicinity, leading to erroneous measurements of rheological quantities [13]. Another possibility is that pre-existing inhomogeneities such as pores in an otherwise rigid material can entrain the tracers, resulting in measurements that underestimate the bulk viscoelasticity of the material in question [5]. To overcome these difficulties, a new method known as two-particle microrheology has been established [13], which looks at the cross-correlated thermal motions of pairs of particles. The correlated motion of two beads is driven by long-wavelength modes in the system, and is therefore independent of the local environment of the tracers. While two-particle microrheology has been applied to 3-D systems [13, 14] where the

strain field decays as  $1/R$ , a formalism for 2-D interfacial systems coupled to viscous bulk fluids has not been experimentally determined to date. This is largely due to the non-trivial nature of the flow field created by the thermal motion of particles at an interface. An understanding of this flow field is critical towards determining the true microrheological behavior of an interface [7, 8, 9].

In this Letter, we look at the correlated motions of particles embedded at an air-water interface in the presence of human serum albumin (HSA) protein molecules. This is done as a function of particle separation  $R$  and lag times  $\tau$ , for correlated motion along the line joining the centers of particles,  $D_{rr}(R, \tau)$ , and motion perpendicular,  $D_{\theta\theta}(R, \tau)$ . The interface is purely viscous, with  $D_{rr}$ ,  $D_{\theta\theta} \sim \tau$ . The correlations show a transition as a function of the surface viscosity  $\eta_s$ ; at high  $\eta_s$  their behavior is 2-D dominated; at intermediate  $\eta_s$  they show crossover behavior; and at low  $\eta_s$  their behavior is strongly influenced by the 3-D fluid reservoirs ( $\sim 1/R$  and  $1/R^2$  respectively). The correlated motion of the tracer particles for different surface viscosities can be scaled onto a single master curve, which agrees with theoretical predictions [15]. The surface viscosity  $\eta_s$  determined from the scaling parameters of the master curve agrees well with  $\eta_s$  from one-particle measurements, demonstrating the homogeneity of HSA at an interface.

We use aqueous solutions of HSA over a narrow range of bulk concentrations ( $c = 0.03 - 0.045$  mg/ml) to obtain our interface. At these bulk concentrations, HSA molecules diffuse to the air-water interface to form a thin monolayer of size  $\sim 3$  nm [16], thereby creating a surface shear viscosity. The surface concentration of HSA slowly increases over time [17], and so the surface shear viscosity  $\eta_s$  can be varied over a wide range. The viscosity of the bulk solution is negligibly different from the viscosity of water, and is assumed to be  $\eta = 1.0$  mPa·s for all our experiments, while the viscosity of air is considered to be negligible. Micron-sized polystyrene beads (Interfacial Dynamics Corporation, carboxyl-modified, radius  $a = 0.9\mu\text{m}$ ) dispersed in an aqueous solution with 20 % isopropyl alcohol, are spread at the interface with a syringe needle to act as

tracer particles. The particles are imaged by bright-field microscopy with a  $20\times$  objective,  $NA=0.45$ , at a spatial resolution of  $606\text{ nm/pixel}$  and a frame rate of  $30\text{ Hz}$ . For each sample, short movies of 200 frames are recorded with a CCD camera (Integrated Design Tools, X-Stream Vision XS-3) that has  $1240 \times 1024$  pixel resolution, with hundreds of particles lying within the field of view. The positions of the tracers for every frame are determined by particle tracking. Of potential concern is the presence of interactions between particles [18], whether due to electrostatic forces, capillary forces, or other origin. For all experiments, we measure the pair correlation function  $g(R)$  and find no structure for the separations  $R$  considered in our results. Also, our experiments are conducted in the dilute particle limit, and a control experiment for one of the surface protein concentrations verifies that our results are unchanged when the particle concentration is varied by a factor of 4. This ensures that long-range particle interactions are not present and do not affect our conclusions.

From the particle positions, we determine the vector displacements of the tracers  $\Delta r_\alpha(t, \tau) = r_\alpha(t + \tau) - r_\alpha(t)$  where  $t$  is the absolute time and  $\tau$  is the lag time. Care is taken to eliminate any global drift of the sample from these vector displacements. We can then calculate the ensemble-averaged cross-correlated particle motions [13]

$$D_{\alpha\beta}(r, \tau) = \langle \Delta r_\alpha^i(t, \tau) \Delta r_\beta^j(t, \tau) \delta[r - R^{ij}(t)] \rangle_{i \neq j, t} \quad (1)$$

where  $i, j$  are particle indices,  $\alpha$  and  $\beta$  represent different co-ordinates and  $R^{ij}$  is the distance between particles  $i$  and  $j$ . In particular, we focus on the diagonal elements of this tensor product:  $D_{rr}$ , which measures the correlated motion along the line joining the centers of particles, and  $D_{\theta\theta}$ , which measures the correlated motion perpendicular to this line (the off-diagonal elements are assumed to be uncorrelated, and hence 0). In addition, we also calculate the one-particle MSD,  $\langle \Delta r^2(\tau) \rangle$ , from the self terms ( $i = j$ ) in the above expression. In 2-D interfacial systems coupled to a bulk fluid reservoir, this one-particle MSD is related to the surface viscosity  $\eta_s$  by a modified Stokes-Einstein relation [10, 11, 12]

$$\langle \Delta r^2(\tau) \rangle = 4D'_s\tau \quad (2)$$

where  $D'_s = D_s [\ln(2\eta_s/\eta_a) - \gamma_E + O(\eta_a/\eta_s)]$ , with  $D_s = k_B T / 4\pi\eta_s$  and  $\gamma_E = 0.577$  being Euler's constant. This equation, derived by Saffman for  $\eta_s/\eta_a \gg 1$  [12], has been modified by Hughes [19] to work in the limit where  $\eta_s/\eta_a \sim 1$ . Equation 2 has been used to describe a variety of homogeneous systems [20] and we use the measured values of  $\langle \Delta r^2(\tau) \rangle$  to solve it for the one-particle surface viscosity,  $\eta_{s,1p}$  (refer inset of Fig. 1 for example).

However, as noted above, one-particle measurements may be inaccurate if the system is heterogeneous, so we perform two-particle measurements to check this, and also to further probe the spatial flow field around the particles. In Fig. 1(a), we show  $D_{rr}$  as a function of  $R$  for different lag times  $\tau$ , for a sample with  $\eta_{s,1p} = 340$

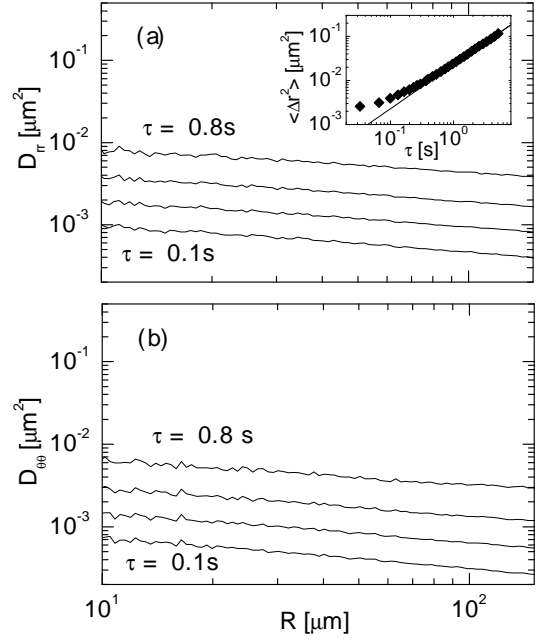


FIG. 1: (a) and (b) Two point correlation functions  $D_{rr}(R, \tau)$  and  $D_{\theta\theta}(R, \tau)$  for a sample with  $\eta_{s,1p} = 340\text{ nPa}\cdot\text{s}\cdot\text{m}$ , with lag times  $\tau = 0.1, 0.2, 0.4$  and  $0.8\text{ s}$ . The evenly spaced correlation functions imply that  $D_{rr}, D_{\theta\theta} \sim \tau$ . Inset: One-particle MSD for the sample (diamonds), where the straight line is a fit giving  $\eta_{s,1p} = 340\text{ nPa}\cdot\text{s}\cdot\text{m}$ , using Eqn. 2.

$\text{nPa}\cdot\text{s}\cdot\text{m}$ . The motion of a tracer particle creates a flow field that affects the motion of other particles. This flow field decays as we move further out from the particle; hence the correlated motions decay as a function of particle separation for all lag times. From the one-particle measurements, we observe that HSA monolayers at an interface are entirely viscous at these surface concentrations, and therefore we also observe that  $D_{rr} \sim \tau$ . This is illustrated in Fig. 1(a) where all the  $D_{rr}$  are spaced evenly on a log-plot for lag times  $\tau = 0.1, 0.2, 0.4$  and  $0.8\text{ s}$ . A similar linear relationship exists for  $D_{\theta\theta}$ , shown in Fig. 1(b). The linear scaling of the correlation functions enables the estimation of  $\tau$ -independent quantities  $\langle D_{rr}/\tau \rangle_\tau$  and  $\langle D_{\theta\theta}/\tau \rangle_\tau$ , which depend only on  $R$ , and have units of a diffusion coefficient.

Changing the surface shear viscosity  $\eta_s$ , has a substantial effect on both  $D_{rr}$  and  $D_{\theta\theta}$ . At high  $\eta_s$ , Fig. 2(a), both  $\langle D_{rr}/\tau \rangle$  and  $\langle D_{\theta\theta}/\tau \rangle$  are nearly equal and constant over the length scales  $10 < R < 150\mu\text{m}$ . At these surface viscosities, the behavior can be considered to be 2-D dominated, where the bulk fluid reservoirs have minimal influence. As  $\eta_s$  is decreased, Fig. 2(b), we see curvature in these functions and deviation between their values, over the same range of length scales. At very low  $\eta_s$ , Fig. 2(c), this deviation is even more pronounced, with  $\langle D_{rr}/\tau \rangle \sim 1/R$  and  $\langle D_{\theta\theta}/\tau \rangle \sim 1/R^2$ . At these viscosities, bulk fluid effects begin to dominate, although the behavior is still 2-D as the protein molecules are confined to an interface. For all surface viscosities, the behavior of

the correlation functions is markedly different from what is seen in bulk 3-D systems (where  $D_{rr}, D_{\theta\theta} \sim 1/R$ ), and is sensitively dependent on  $\eta_s$ . Despite the differences

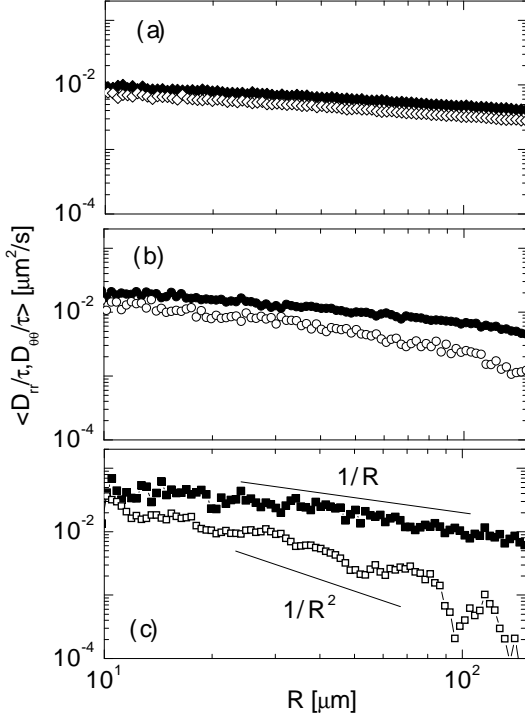


FIG. 2: Correlation functions  $\langle D_{rr}/\tau \rangle$  (solid symbols) and  $\langle D_{\theta\theta}/\tau \rangle$  (open symbols) as a function of particle separation  $R$ , for decreasing surface viscosities  $\eta_s$ . The samples are a) 2-D dominated:  $\eta_{s,1p} = 340$  nPa·s·m (diamonds), b) Crossover:  $\eta_{s,1p} = 72$  nPa·s·m (circles), c) 3-D dependent:  $\eta_{s,1p} = 21.3$  nPa·s·m (squares).

in the behavior of  $\langle D_{rr}/\tau \rangle$  and  $\langle D_{\theta\theta}/\tau \rangle$  at low and high surface viscosities, all the data can be scaled onto a single master curve. We define dimensionless correlation functions  $\bar{D}_{rr,\theta\theta} = \langle D_{rr,\theta\theta}/\tau \rangle / 2D_s$  and a reduced separation  $\beta = R/L$ , where  $L = \eta_s/\eta$ . Both scale factors  $L$  and  $D_s$  depend only on  $\eta_s$ ; however, we allow them to vary independently to obtain two independent measures of  $\eta_s$  ( $\eta'_s$  and  $\eta''_s$  respectively, in other words,  $\beta = R\eta/\eta'_s$ , and  $D_s = k_B T / 4\pi\eta''_s$ ). Fig. 3 shows the scaled variables  $\bar{D}_{rr}$ ,  $\bar{D}_{\theta\theta}$  plotted against the scaled separation  $\beta$ . All the data sets fall on a single master curve, that spans nearly 4 orders of magnitude. This master curve has the characteristics of the individual data sets: at small  $\beta$  ( $\beta \ll 1$ ), the curves are nearly logarithmic, at intermediate  $\beta$  ( $\beta \approx 1$ ), they show crossover behavior, while at large  $\beta$  ( $\beta \gg 1$ ), they show behavior that asymptotically approaches  $1/R$  and  $1/R^2$  for  $\bar{D}_{rr}$  and  $\bar{D}_{\theta\theta}$  respectively. The solid lines are fits obtained from theoretical calculations of the response of an interface to an in-plane point force [10, 15], and have the form

$$\begin{aligned} \bar{D}_{rr} &= [\frac{\pi}{\beta} H_1(\beta) - \frac{2}{\beta^2} - \frac{\pi}{2}(Y_0(\beta) + Y_2(\beta))] \\ \bar{D}_{\theta\theta} &= [\pi H_0(\beta) - \frac{\pi}{\beta} H_1(\beta) + \frac{2}{\beta^2} - \frac{\pi}{2}(Y_0(\beta) - Y_2(\beta))](3) \end{aligned}$$

where the  $H_\nu$  are Struve functions, and the  $Y_\nu$  are Bessel functions of the second kind. More importantly, up to a scale factor, Eqn. 3, and therefore the master curve, also characterizes the spatial dependence of the flow field at an interface in response to a perturbation, such as thermal motion of tracers. To our knowledge, this is the first experimental mapping of this flow field over such a wide range of length scales. The inset to Fig. 3 de-

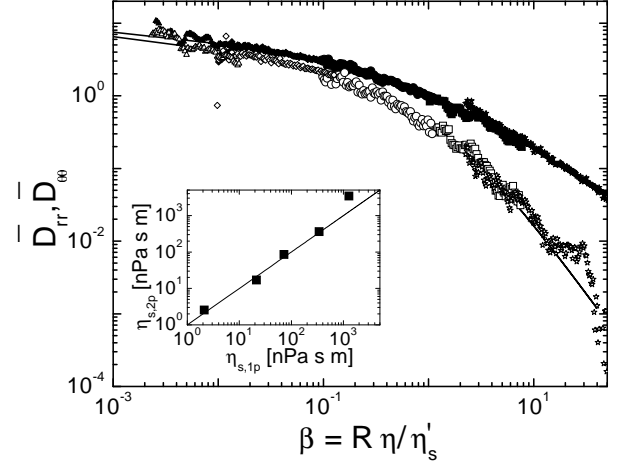


FIG. 3: Master curve of scaled variables  $\bar{D}_{rr}$  (solid symbols) and  $\bar{D}_{\theta\theta}$  (open symbols) as a function of reduced particle separation  $\beta$ . Symbols are same as in Fig. 2, with two additional data sets ( $\eta_{s,1p} = 2.1$  nPa·s·m; stars and  $\eta_{s,1p} = 1275$  nPa·s·m; triangles). Solid lines represent theoretical fits to the data. Inset: One- and two-particle surface viscosities for the five samples shown in the master curve. The straight line has a slope of 1, indicating an equality between the two viscosities.

scribes the scale factors used to create the master curve. For all the samples, the two independent estimates of the two-particle viscosity,  $\eta'_s$  and  $\eta''_s$ , are within 15% of each other; we therefore plot their average,  $\eta_{s,2p}$ , against the one particle viscosity  $\eta_{s,1p}$ . For most of the samples, the one- and two-particle measurements agree reasonably well with each other. However, at the highest viscosity, and therefore, the highest surface concentration of HSA, the two measurements deviate well beyond our experimental error. We believe this is a consequence of heterogeneity in the system; one possibility could be the formation of condensed phases at the interface at such high surface concentrations of HSA. While this would explain the underestimation of the true surface viscosity by the one-particle measurement, such an assumption deserves further study.

Conventional microrheology uses the one-particle MSD,  $\langle \Delta r^2(\tau) \rangle$ , to determine  $G'(\omega)$  and  $G''(\omega)$  [3]; these quantities are directly compared to bulk rheological measurements. Since the one-particle measurements are inherently local in nature, a more accurate approach is to determine the two-particle MSD [13],  $\langle \Delta r^2(\tau) \rangle_D$ . Analogous to [13], we calculate this quantity for our 2-D vis-

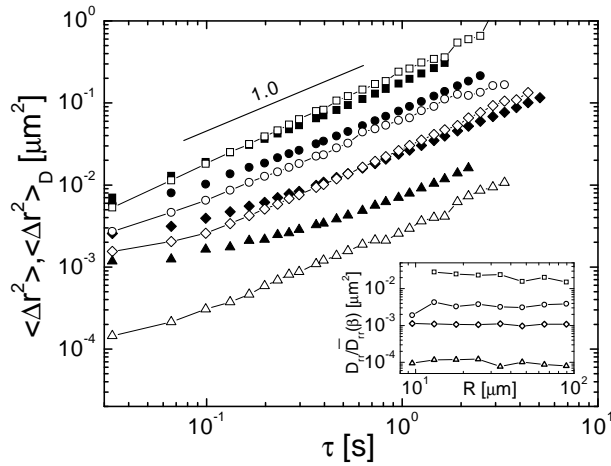


FIG. 4: One-particle (solid symbols) and two-particle (open symbols) MSDs for four of the five samples shown in Fig.3. Inset: radial scaling of  $D_{rr}$  for the different samples at a lag time  $\tau = 0.53$ s.

cous systems by extrapolating the long wavelength fluctuations of the medium to the bead size, which gives

$$\langle \Delta r^2(\tau) \rangle_D = 2 \left( \frac{D_{rr}(R, \tau)}{D_{rr}(\beta)} \right)_R [\ln(2\eta_s/\eta a) - \gamma_E + O(\eta a/\eta_s)] \quad (4)$$

This expression can readily be generalized for viscoelastic interfaces, i.e., with a non-zero  $G'(\omega)$ ; however, such measurements are beyond the scope of this study. In practice, we confirm that  $D_{rr}(R, \tau)/\bar{D}(\beta)$  is nearly constant over the length scales studied,  $9 < R < 100 \mu\text{m}$ , shown in the inset to Fig. 4 for a specific lag time ( $\tau = 0.53$ s). The averaged quantity  $\langle D_{rr}(R, \tau)/\bar{D}(\beta) \rangle_R$  is then calculated for all lag times to obtain  $\langle \Delta r^2(\tau) \rangle_D$ . From Fig. 4, we see that for all the samples,  $\langle \Delta r^2(\tau) \rangle_D$  is purely diffusive, as expected for a viscous system. At short lag times, the

turnover in the one-particle MSDs, caused by resolution-limited noise, is significantly reduced in the two-particle MSDs. Finally, at long lag times,  $\langle \Delta r^2(\tau) \rangle_D$  is equal to  $\langle \Delta r^2(\tau) \rangle$  within experimental error, except for the highest viscosity (as expected, since  $\eta_{s,1p}$  deviates from  $\eta_{s,2p}$  for this sample). These observations provide conclusive evidence of the accuracy of two-particle measurements over local probes of the rheology.

The verification of two-point microrheological techniques for a quasi-2D systems has applications for the study of inhomogeneous materials at an interface. Any significant variation between  $\langle \Delta r^2(\tau) \rangle_D$  and  $\langle \Delta r^2(\tau) \rangle$  indicates the presence of heterogeneities, and the estimation of rheological quantities from the motion of tracer particles can be modified to reflect this. Future work will involve studying lipid molecules at an interface under compression/expansion, which creates domains such as liquid expanded or liquid condensed phases. We expect that our two-particle measurements will provide accurate measurements of the surface viscosity even with the presence of these heterogeneities. Other possible areas of future research are biological interfaces such as cell membranes, with the diffusing entities being protein aggregates or lipid rafts. However, two-particle microrheology can only probe heterogeneities of the order of the bead size and above, which may not always be applicable for lipid systems with molecules in the nanometer scale. It should also be pointed out that for cases where  $\eta_s$  is very small, the correlation functions ( $D_{\theta\theta}$  in particular) die out rapidly, making an estimation of  $\eta_{s,2p}$  from the two-particle measurements difficult. However, one-particle microrheology is equally inaccurate in this limit, as the bulk viscosity will dominate over surface effects, making such measurements challenging. Nonetheless, it would be extremely interesting to test the limits of the scaling behavior in this regime.

- 
- [1] A. Einstein, Ann. Phys. **17**, 549 (1905).
  - [2] W. Sutherland, Phils. Mag. **9**, 781 (1905).
  - [3] T. G. Mason and D. A. Weitz, Phys. Rev. Lett. **74**, 1250 (1995).
  - [4] B. R. Dasgupta and D. A. Weitz, Phys. Rev. E. **71**, 021504 (2005).
  - [5] M. L. Gardel et al., Phys. Rev. Lett. **91**, 158302 (2003).
  - [6] C. Y. Xu, V. Breedveld, and J. Kopecek, Biomacromolecules **6**, 1739 (2005).
  - [7] M. Sickert and F. Rondelez, Phys. Rev. Lett. **90**, 126104 (2003).
  - [8] A. Pralle et al., J. Cell. Bio. **148**, 997 (2000).
  - [9] Y. Gambin et al., Proc. Natl. Acad. Sci. USA **103**, 2098 (2006).
  - [10] H. A. Stone and A. Ajdari, J. Fluid. Mech. **369**, 151 (1998).
  - [11] T. M. Fischer, J. Fluid. Mech. **498**, 123 (2004).
  - [12] P. G. Saffman and M. Delbrück, Proc. Natl. Acad. Sci. USA **72**, 3111 (1975).
  - [13] J. C. Crocker et al., Phys. Rev. Lett. **85**, 888 (2000).
  - [14] A. J. Levine and T. C. Lubensky, Phys. Rev. Lett. **85**, 1774 (2000).
  - [15] A. J. Levine and F. C. MacKintosh, Phys. Rev. E. **66**, 061606 (2002).
  - [16] J. R. Lu, T. J. Su, and J. Penfold, Langmuir **15**, 6975 (1999).
  - [17] P. Chen et al., Colloids And Surfaces B-Biointerfaces **6**, 279 (1996).
  - [18] R. Aveyard et al., Phys. Rev. Lett. **88**, 246102 (2002).
  - [19] B. D. Hughes, B. A. Pailthorpe and L. R. White, J. Fluid. Mech. **110**, 349 (1981).
  - [20] R. Peters and R. J. Cherry, Proc. Natl. Acad. Sci. USA **79**, 4317 (1982); W. L. C. Vaz, F. Goodsaid-Zalduondo, and K. Jacobson, FEBS Lett. **174**, 199 (1984); W. L. C. Vaz, R. M. Clegg, and D. Hallmann, Biochemistry **24**, 781 (1985).